
Environmental Disturbances

The undesirable motion of a ship in a seaway is induced by the action of environmental disturbances: waves, wind and current. For the particular ship motion control problem considered in this book (course keeping and roll stabilisation), ocean waves are the dominant environmental disturbance; and hence, the type of disturbances described in this chapter.

From the control system design perspective, the characterization of the disturbances acting on the ship is essential to design good performance ship motion controllers and to understand limitations that may prevent the design achieving the performance specifications. In this chapter, we review models and simulation techniques that characterize the elevation of the sea surface. This serves as a basis for the study of ship motion: response to wave excitation loads—which is covered in Chapter 4.

2.1 Basic Hydrodynamic Assumptions

The description of waves and the interaction between waves and floating objects requires some basic knowledge of fluid flow behaviour. This is the field of study of hydrodynamics. In this section, we review some the elementary concepts.

2.1.1 Fluid Flow and Continuity

To describe most fluid flow phenomena associated with the waves and the motion of ships in waves, we need to know the velocity of the fluid and the pressure at different locations. The velocity of the fluid at the location

$$\mathbf{x} = [x_1, x_2, x_3]^T \quad (2.1)$$

is given by the *fluid flow velocity vector*:

$$\mathbf{v}(\mathbf{x}, t) = [v_1(\mathbf{x}, t), v_2(\mathbf{x}, t), v_3(\mathbf{x}, t)]^T. \quad (2.2)$$

This vector is described relative to the, so-called, hydrodynamic reference frame (*h*-frame) that has its origin in the mean free surface of the water with the vertical coordinate z taken positive upwards.

For the flow velocities involved in ship motion, the fluid can be considered *incompressible*, i.e. of constant density ρ . Under this assumption, the net volume rate at a volume V enclosed by a closed surface S is

$$\iint_S \mathbf{v} \cdot \mathbf{n} \, ds = \iiint_V \mathbf{div}(\mathbf{v}) \, dV = 0, \quad (2.3)$$

where we have used the divergence theorem—see [3] for different identities derived from (2.3). Since (2.3) is valid for all the regions V in the fluid, then by assuming that $\nabla \cdot \mathbf{v}$ is continuous, we obtain

$$\mathbf{div}(\mathbf{v}) = \nabla \cdot \mathbf{v} = \frac{\partial v_1}{\partial x} + \frac{\partial v_2}{\partial y} + \frac{\partial v_3}{\partial z} = 0, \quad (2.4)$$

which is the *continuity equation* for incompressible flows.

2.1.2 Material Derivative

Let $f(x, y, z, t)$ be a scalar function and $\mathbf{f}(t, x, y, z)$ a vector function, which describe some properties of interest of the fluid; then,

$$\begin{aligned} \frac{df}{dt} &= \frac{\partial f}{\partial t} + \frac{\partial f}{\partial x} \frac{dx}{dt} + \frac{\partial f}{\partial y} \frac{dy}{dt} + \frac{\partial f}{\partial z} \frac{dz}{dt} \\ \frac{d\mathbf{f}}{dt} &= \frac{\partial \mathbf{f}}{\partial t} + \frac{\partial \mathbf{f}}{\partial x} \frac{dx}{dt} + \frac{\partial \mathbf{f}}{\partial y} \frac{dy}{dt} + \frac{\partial \mathbf{f}}{\partial z} \frac{dz}{dt}. \end{aligned} \quad (2.5)$$

If these are taken for the function $\mathbf{x}(t)$ s.t. $\dot{\mathbf{x}}(t) = \mathbf{v}(t)$, then we have a special notation, and the derivatives are called *material derivatives*:

$$\begin{aligned} \frac{Df}{Dt} &= \frac{\partial f}{\partial t} + \frac{\partial f}{\partial x} v_1 + \frac{\partial f}{\partial y} v_2 + \frac{\partial f}{\partial z} v_3 \\ \frac{D\mathbf{f}}{Dt} &= \frac{\partial \mathbf{f}}{\partial t} + \frac{\partial \mathbf{f}}{\partial x} v_1 + \frac{\partial \mathbf{f}}{\partial y} v_2 + \frac{\partial \mathbf{f}}{\partial z} v_3, \end{aligned} \quad (2.6)$$

or

$$\frac{Df}{Dt} = \frac{\partial f}{\partial t} + \mathbf{v} \cdot \nabla f, \quad \frac{D\mathbf{f}}{Dt} = \frac{\partial \mathbf{f}}{\partial t} + (\mathbf{v} \cdot \nabla) \mathbf{f}. \quad (2.7)$$

The first terms on the right-hand side account for the rate of change at a fixed location, whereas the second terms account for the rate of change following the fluid at the local flow velocity $\mathbf{v}(t)$.

2.1.3 Navier-Stokes Equations

The conservation of momentum in the flow is described by the *Navier-Stokes Equations* (see, for example, [3])

$$\rho \frac{D\mathbf{v}}{Dt} = \rho \mathbf{F} - \nabla p + \mu \nabla^2 \mathbf{v}, \quad (2.8)$$

where \mathbf{F} are accelerations due to volumetric forces, from which only the gravity it is often considered; *i.e.* $\mathbf{F} = [0 \ 0 \ -g]^T$, $p = p(\mathbf{x}, t)$ is the pressure, and μ is the viscosity coefficient of the fluid.

To describe the real flow of ships, it is then necessary to solve the Navier-Stokes equations (2.8) together with the continuity equation (2.4). These form a system of non-linear partial differential equations, which unfortunately, do not have analytical solution, and the numerical solutions are still far from being feasible with current computing power. One approximation used consists in decomposing the unknowns, \mathbf{v} and p , into a steady part which is a time average and a fluctuating part. This gives rise to the Reynolds Averaged Navier-Stokes equations (RANS), which can be solved numerically [23].

2.1.4 Potential Flows and The Bernoulli Equation

If we neglect viscosity, we have what we call an *ideal fluid*. This is a commonly made assumption to calculate ship flows because viscosity often matters only in a thin layer close to the ship hull. By disregarding the last term in (2.8), we obtain the *Euler* equations of fluid motion:

$$\rho \frac{D\mathbf{v}}{Dt} = \rho \mathbf{F} - \nabla p. \quad (2.9)$$

A further simplification of the flow description is obtained by assuming that the flow is *irrotational*, this is

$$\mathbf{curl}(\mathbf{v}) = \nabla \times \mathbf{v} = 0. \quad (2.10)$$

The term *potential flow* is used to describe irrotational flows of inviscid-incompressible fluids. Under this assumption, there exists a scalar function $\Phi(t, x, y, z)$ called *potential* such that

$$\mathbf{v} = \nabla \Phi. \quad (2.11)$$

Hence, if we know the potential, we can calculate the velocities:

$$v_1 = \frac{\partial \Phi}{\partial x}, \quad v_2 = \frac{\partial \Phi}{\partial y}, \quad v_3 = \frac{\partial \Phi}{\partial z}. \quad (2.12)$$

For this case, the continuity equation reverts to the Laplace Equation of the potential:

$$\nabla^2 \Phi = \frac{\partial^2 \Phi}{\partial x^2} + \frac{\partial^2 \Phi}{\partial y^2} + \frac{\partial^2 \Phi}{\partial z^2} = 0. \quad (2.13)$$

The potential can then be obtained by solving the Laplace equation (2.13) subject to appropriate boundary conditions, *i.e.* by solving a boundary value problem.

The Euler equation of fluid motion (2.9) can be expressed as

$$\frac{\partial \mathbf{v}}{\partial t} + (\mathbf{v} \cdot \nabla) \mathbf{v} = -\nabla \left(\frac{p}{\rho} + \mathcal{R} \right), \quad (2.14)$$

where $-\nabla \mathcal{R} = \mathbf{F}$, *i.e.* $\mathcal{R} = gz$. Using properties of vector calculus (see, for example, [3]), this becomes

$$\frac{\partial \mathbf{v}}{\partial t} + (\nabla \times \mathbf{v}) \times \mathbf{v} = -\nabla \left(\frac{p}{\rho} + \frac{1}{2} \mathbf{v}^2 + \mathcal{R} \right) \quad (2.15)$$

If the flow is irrotational, then the second term of the left-hand side vanishes, and we can express the above as

$$\nabla \left(\frac{p}{\rho} + \frac{\partial \Phi}{\partial t} + \frac{1}{2} (\nabla \Phi)^2 + \mathcal{R} \right) = 0. \quad (2.16)$$

This expression is valid in the whole fluid. Hence,

$$\frac{p}{\rho} + \frac{\partial \Phi}{\partial t} + \frac{1}{2} (\nabla \Phi)^2 + gz = C, \quad (2.17)$$

which is the *Bernoulli equation*.

By setting the constant $C = p_0/\rho$, we can obtain the relative pressure from

$$p - p_0 = -\rho gz - \rho \frac{\partial \Phi}{\partial t} - \rho (\nabla \Phi)^2. \quad (2.18)$$

For simplicity, the atmospheric pressure p_0 is often considered zero.

Potential flows offer a great simplification, which can be seen from (2.11) and (2.18), *i.e.* if we know the potential, then we know the velocity and the pressure in the fluid, from which we can calculate the forces acting on a floating body. For *most* problems related ship motion in waves, potential theory is sufficient to obtain results with appropriate accuracy for engineering purposes. For further discussions on the topics presented in this section, see [3], [23], [63], [114] and [159].

2.2 Regular Waves in Deep Water

The term *regular wave* refers to a harmonic wave travelling on the surface of the fluid:

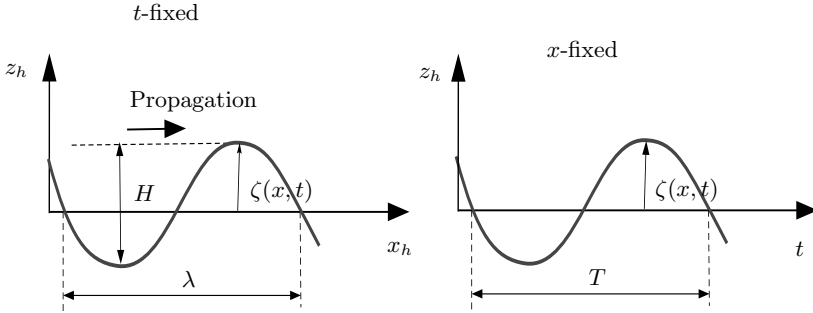


Fig. 2.1. Regular wave parameters.

$$\zeta(x, t) = \bar{\zeta} \sin(\omega t - kx + \varepsilon). \quad (2.19)$$

Figure 2.1 depicts the main parameters defining a harmonic wave traveling in the x -direction with respect to the hydrodynamic reference frame (x_h, y_h, z_h) . The sea surface elevation is denoted by $\zeta(x, t)$. This is characterised by a sinusoid of constant amplitude $\bar{\zeta}$ as described in (2.19). The *double amplitude* or *wave height* is denoted by $H = 2\bar{\zeta}$, λ is the *wave length*, and ω is the circular *wave frequency* related to the wave period T via $\omega = 2\pi/T$. The speed at which the crest of the wave travels over the surface is called the *wave celerity* $c = \lambda/T$.

A mathematical description of the fluid flow velocities and the pressure distribution due to a travelling wave can be obtained from potential theory. Indeed, if $\Phi_w(t, x, y, z)$ is the potential due to the traveling wave, then, the following equation is satisfied in the fluid:

$$\nabla^2 \Phi_w = 0. \quad (2.20)$$

By solving this, the velocity of the fluid particles is given by $\nabla \Phi_w$, and the pressure can be calculated from the Bernoulli equation (2.18).

To obtain the potential, we need to solve Equation (2.20) together with the following boundary conditions (see, for example, [63]):

1. **Kinematic free-surface boundary condition.** This condition establishes that a fluid particle on the free surface remains on the free surface. Mathematically, this is expressed through the material derivative $D(z - \zeta(x, y, t))/Dt = 0$. Using a Taylor expansion and taking only the linear terms, this condition becomes

$$\frac{\partial \zeta}{\partial t} = \frac{\partial \Phi_w}{\partial z} \quad \text{on} \quad z = 0. \quad (2.21)$$

2. **Dynamic free-surface condition.** This condition establishes that the water pressure equals the atmospheric pressure on the free surface. By considering the linear terms in the Bernoulli equation (2.18), this condition becomes

$$g\zeta + \frac{\partial \Phi_w}{\partial t} = 0 \quad \text{on} \quad z = 0. \quad (2.22)$$

3. **Sea bed condition.** This condition establishes that there is no flow velocity component normal to the sea bottom. Assuming a flat sea bed this is

$$\frac{\partial \Phi_w}{\partial z} = 0 \quad \text{on} \quad z = -h, \quad (2.23)$$

where h is the depth.

The solution of the above boundary value problem with $h \rightarrow \infty$ that is consistent with the physics of the problem for a wave propagating in the x_h direction is [159, 63, 3]

$$\Phi_w(t, x, y, z) = \frac{g\bar{\zeta}}{\omega} e^{kz} \cos(\omega t - kx + \varepsilon). \quad (2.24)$$

The parameter $\bar{\zeta}$ is the amplitude of the wave, ε is the initial phase and k is the *wave number*. For the deep water conditions being considered ($h \geq \lambda/2$), the following *dispersion relationships* hold:

$$k = \frac{\omega^2}{g} \quad \lambda = \frac{g}{2\pi} T^2. \quad (2.25)$$

Also, the fact that only the linear terms are considered in the free-surface boundary conditions means that the solution will be valid for waves of small steepness, *i.e.* $\bar{\zeta}/\lambda \ll 1$ (see [3]).

If the waves propagate at an angle χ with respect to the positive axis x_h , then the potential can be expressed as

$$\Phi_w(t, x, y, z) = \frac{g\bar{\zeta}}{\omega} e^{kz} \cos(\omega t - kx \cos(\chi) - ky \sin(\chi) + \varepsilon). \quad (2.26)$$

From the dynamic free-surface condition, we obtain the wave elevation:

$$\zeta(x, y, t) = \bar{\zeta} \sin[\omega t + \varepsilon - kx \cos(\chi) - ky \sin(\chi)]. \quad (2.27)$$

Also, $\nabla \Phi_w$ gives the velocity components of a particle in the fluid:

$$\begin{aligned} v_1(x, y, z, t) &= \omega \cos(\chi) e^{kz} \bar{\zeta} \sin[\omega t + \varepsilon - kx \cos(\chi) - ky \sin(\chi)] \\ v_2(x, y, z, t) &= \omega \sin(\chi) e^{kz} \bar{\zeta} \sin[\omega t + \varepsilon - kx \cos(\chi) - ky \sin(\chi)] \\ v_3(x, y, z, t) &= \omega e^{kz} \bar{\zeta} \cos[\omega t + \varepsilon - kx \cos(\chi) - ky \sin(\chi)] \end{aligned} \quad (2.28)$$

The behaviour of waves is significantly affected by the depth. For the particular applications considered in this book, only deep water characteristics

will be considered. Shallow water effects are discussed, for example, in [159, 163].

The wave description presented above corresponds to the, so-called, first-order wave theory or linear wave theory. The linearity follows from the Laplace equation and the boundary conditions considered: the principle of superposition holds for the potentials; and thus, for the surface elevation and fluid particle velocities. Second-order theory, for example, accounts for non-linearities related to the square of the wave amplitude. This gives a more accurate description of mean drift forces and slowly-varying wave induced loads on ships and marine structures, which is important for the analysis of moored ships and structures and to evaluate added resistance in waves [63, 23]. First-order wave theory only describes zero mean phenomena, and this is sufficient for the problems of autopilot and fins stabiliser control design.

2.3 Encounter Frequency

In the previous section, we have described regular waves from a stationary reference frame. When the ship is at zero speed, the frequency at which the waves excite the ship coincides with the wave frequency; and thus, the previous description is valid. However, when the ship moves, the frequency observed from the ship differs from the wave frequency. The frequency experienced by the ship is called the *encounter frequency*, and it is denoted by ω_e .

If the ship moves forwards with an average speed U , the sea can be more conveniently described relative to a frame (o_h, x_h, y_h) that moves at the average speed of the vessel as shown in Figure 2.2. This figure also shows the adopted convention for the, so-called, *encounter angle* χ , and also the usual denomination for the different sailing conditions:

- Following seas ($\chi = 0$ or 360 deg),
- Quartering seas ($0 < \chi < 90$ deg or $270 < \chi < 360$ deg),
- Beam seas ($\chi = 90$ deg—port or 270 deg—starboard),
- Bow seas ($90 < \chi < 180$ deg or $180 < \chi < 270$ deg),
- Head seas ($\chi = 180$ deg).

From Figure 2.2, it follows that the relative speed at which the waves overtake the ship is $c - U \cos(\chi)$. Then, we can express the encounter frequency as

$$\omega_e = \frac{2\pi}{T_e} = \frac{2\pi}{\lambda} [c - U \cos(\chi)],$$

or

$$\omega_e = \omega - \frac{\omega^2 U}{g} \cos(\chi). \quad (2.29)$$

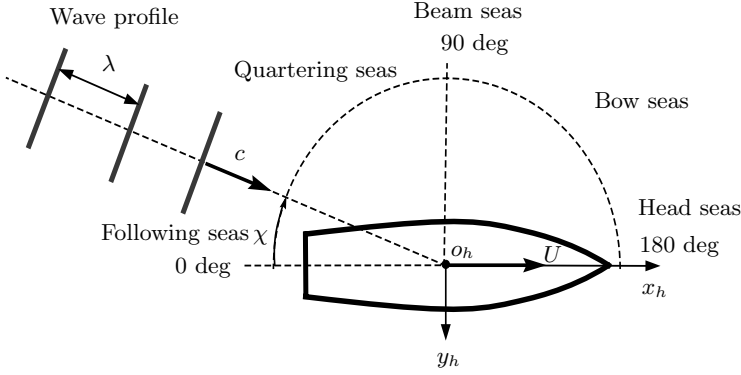


Fig. 2.2. Encounter angle definition and usual denomination for sailing conditions.

Expression (2.29) represents the transformation in frequency that a regular wave goes through when it is observed either from a stationary frame or from a frame moving with the forward speed of the vessel. Figure 2.3 shows a schematic representation of the transformation between ω and ω_e . From this figure, we can see that when the vessel is sailing in bow or head seas the wave frequencies are mapped into higher frequencies. In beam seas, however, there is no change and both ω and ω_e are the same. In following and quartering seas, the situation becomes more involved as different wave frequencies can be mapped into the same encounter frequency.

From the development in the previous section, we can also see that long waves travel faster than short waves in deep water:

$$c = \sqrt{\frac{g\lambda}{2\pi}}. \quad (2.30)$$

Hence, in following and quartering seas, long waves overtake the vessel whereas short waves are overtaken by the vessel. Indeed, for $0 < \omega < \frac{g}{U \cos(\chi)}$ the waves overtake the vessel. The wave frequency $\omega = \frac{g}{U \cos(\chi)}$, at which $\omega_e = 0$, corresponds to the situation in which the component of the ship velocity in the direction of wave propagation is the same as the wave celerity. In this case, the wave pattern observed from the ship remains stationary and travels along with the ship. Finally, for high-frequency waves, the encounter frequency is negative, meaning that the ship overtakes the waves.

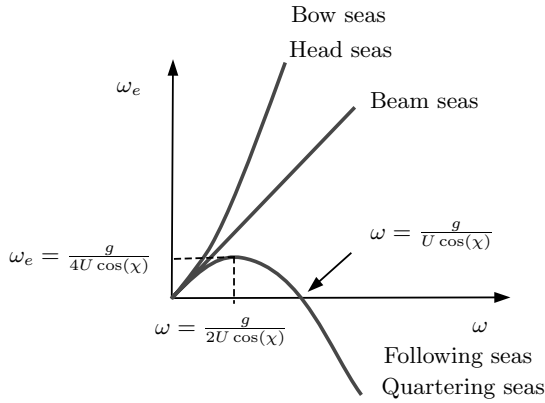


Fig. 2.3. Transformation from wave to encounter frequency under different sailing conditions for U fixed.

The motion of a ship in waves is the result of the wave excitation due to the varying distribution of pressure on the hull. From the material presented in this section, it can be envisaged that the wave excitation, as well as the vessel response, will depend not only on the characteristics of the waves—amplitude and frequency—but also on the *sailing conditions*: encounter angle and speed.

2.4 Ocean Waves and Wave Spectra

Ocean waves are random in both time and space. These characteristics are often summarised by the term *irregular* in the marine literature. The stochastic description is, therefore, the most appropriate approach to characterise them. In practice, it is usually assumed that the variations of a stochastic nature of the sea are much slower than the variations of the sea surface itself—stationarity is assumed. Due to this assumption, the elevation of the sea, $\zeta(x, y, t)$, at a position x, y , can be considered a realisation of a stationary stochastic process. The following simplifying assumptions regarding the underlying stochastic model are usually made [99, 213]:

- The observed sea surface, at a certain location and for short periods of time, is considered a realisation of a stationary and homogeneous zero mean Gaussian stochastic process.
- A standard formula for the Power Spectral Density (PSD) of the wave sea surface elevation, $S_{\zeta\zeta}(\omega)$, is adopted. This PSD is commonly referred to as *wave spectrum*, and describes how the energy of the sea surface is distributed in the frequency domain. Under a Gaussian assumption, the process, in a statistical sense, is completely characterised by the PSD $S_{\zeta\zeta}(\omega)$.

The above implies that

$$\begin{aligned}\mathbf{E}[\zeta(t)] &= 0 \\ \mathbf{E}[\zeta(t)^2] &= \int_0^\infty S_{\zeta\zeta}(\omega) d\omega.\end{aligned}\tag{2.31}$$

The validity of the hypotheses of stationarity and Gaussianity has been investigated via extensive analysis of time series recorded from wave-riding buoys. For example, [99] report the following results from studies performed in the North Atlantic Ocean:

- For low and moderate sea states (significant wave height¹ $H_{1/3} < 4$ m), the sea can be considered stationary for periods over 20 min. For more severe sea states, stationarity can be questioned even for periods of 20 min.
- For medium states ($4 < H_{1/3} < 8$ m), Gaussian models are still accurate, but deviations from Gaussianity slightly increase with the increasing severity of the sea state.

The deviations from Gaussianity are related to the severity of the sea state and the depth. If the water is sufficiently deep, however, the sea surface elevation can be considered Gaussian regardless of the sea state [163].

In some applications, the wave slope spectrum may be necessary; this refers to the spacial derivative. For example, for the regular wave described by (2.19), the *wave slope* is given by

$$\zeta'(t, x) = \frac{d\zeta(t, x)}{dx} = -k\bar{\zeta} \cos(\omega t - kx + \varepsilon).\tag{2.32}$$

From this, it follows that the *wave slope spectrum* is given by (see [133])

$$S'_{\zeta\zeta}(\omega) = k^2 S_{\zeta\zeta}(\omega) = \frac{\omega^4}{g^2} S_{\zeta\zeta}(\omega).\tag{2.33}$$

In the case of roll and pitch motion of ships, it is the slope of the waves rather than the height what excites the motion; and due to this the roll and pitch frequency responses are often given relative to the wave slope rather than the amplitude—we will further comment on this in Chapter 4.

¹Average of the heights of largest 1/3rd of the waves.

2.4.1 Statistics of Wave Period

Let us assume that the waves propagate in one direction, so the spectrum depends on the frequency only, *i.e.* $S_{\zeta\zeta}(\omega)$ (this assumption will be removed in a later section). The statistical moments of the spectrum (or spectral moments) of order n of the process $\zeta(t)$ are defined as

$$m_{\zeta}^n = \int_0^{\infty} \omega^n \mathbf{S}_{\zeta\zeta}(\omega) d\omega. \quad (2.34)$$

The moments of the spectrum are used to define several quantities related to the statistics of wave period. Rice [186, 187] showed that for Gaussian processes the following relationships hold:

- **Average wave period** (1/average frequency of the spectrum)

$$\bar{T} \quad \text{or} \quad T_1 = 2\pi \frac{m_{\zeta}^0}{m_{\zeta}^1}. \quad (2.35)$$

- **Zero-crossing wave period** (average period of zero up-crossings)

$$T_z = 2\pi \sqrt{\frac{m_{\zeta}^0}{m_{\zeta}^2}}. \quad (2.36)$$

- **Average period between response maxima** (crests)

$$T_c = 2\pi \sqrt{\frac{m_{\zeta}^2}{m_{\zeta}^4}}. \quad (2.37)$$

Note that the 2π factor in the expressions above appears only if the moments are calculated using a PSD given in terms of the circular frequency (2.34). For a discussion on the units of the PSD, see Section 2.4.3.

2.4.2 Statistics of Maxima

The Gaussian assumption for the sea surface elevation implies that the elevation is statistically symmetrical with respect to the zero level. This assumption also implies that the maxima and minima of a wave record (or realisation) are statistically symmetrical about the zero level. Practical wave records usually present short-period oscillations on top of long-period oscillations. Therefore, we can expect to have more than one maximum within a positive excursion of the realisation, which implies that there will be also positive minima.

A maximum of a realization of a stochastic process $\zeta(t)$ occurs when the realisation of $\dot{\zeta}(t)$ is zero and the realisation $\ddot{\zeta}(t)$ is negative simultaneously.

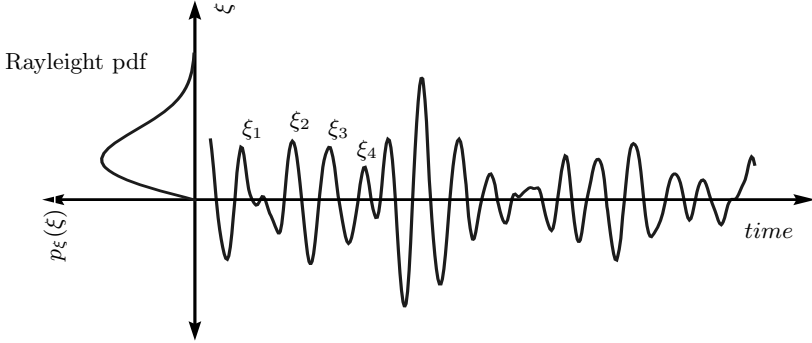


Fig. 2.4. Illustration of statistics of maxima of a narrow banded Gaussian process.

The information about the distribution of the maxima can then be obtained from the joint probability functions of $\zeta(t)$, $\dot{\zeta}(t)$ and $\ddot{\zeta}(t)$. If the maxima are modeled as realisations of a random variables ξ , the probability density function (pdf) $p_\xi(\xi)$ depends on the value of the so-called *spectral broadness*:

$$\epsilon = \sqrt{1 - \frac{T_c}{T_z}}. \quad (2.38)$$

For $\epsilon \approx 0$, *i.e.* $T_c \approx T_z$, there are no multiple maxima and minima within an excursion above or below zero; then, the spectrum is referred to as *narrow banded*. For this case, $p_\xi(\xi)$ can be approximated by a Rayleigh pdf with parameter $b = \sqrt{m_\zeta^0}$. That is,

$$p_\xi(\xi) = \frac{\xi}{m_\zeta^0} \exp\left(\frac{-\xi^2}{2m_\zeta^0}\right) \quad \text{if } \epsilon = 0. \quad (2.39)$$

This case is illustrated in Figure 2.4. When $\epsilon \rightarrow 1$, *i.e.* $T_c \ll T_z$, there is a large number of maxima and minima within an excursion of the realisation of the process above or below zero; then, the spectrum is referred to as *broad banded*, and $p_\xi(\xi)$ is Gaussian. See [182] for details. Except for the two cases mentioned above, the pdf of maxima is neither Rayleigh nor Gaussian; this pdf is given by the, so-called, Rice Distribution—see [182] and [155].

Using the Rayleigh pdf to describe the statistics of maxima of the wave elevation realisations, we can calculate the probability of exceeding a particular wave height. One statistic of particular interest is the average of the $1/n$ -th highest observations of the peaks of the random process. The probability of exceeding an amplitude $\xi_{1/n}$ is given by

$$\mathbf{Pr}[\xi > \xi_{1/n}] = \frac{1}{n} = \int_{\xi_{1/n}}^{\infty} \frac{\xi}{m_\zeta^0} \exp\left(\frac{-\xi^2}{2m_\zeta^0}\right) d\xi. \quad (2.40)$$

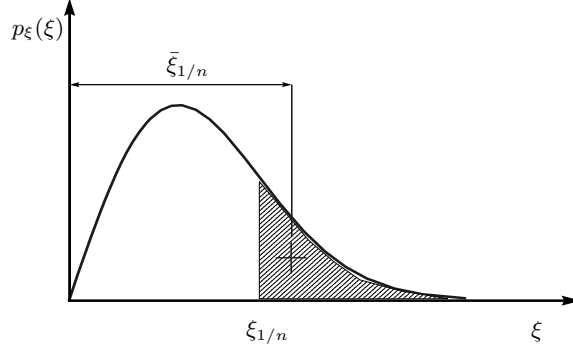


Fig. 2.5. Definition of $1/n$ -th highest observation.

Then, the average of the $1/n$ -th highest observations is defined as

$$\bar{\xi}_{1/n} = n \int_{\xi_{1/n}}^{\infty} \frac{\xi^2}{m_{\xi}^0} \exp\left(\frac{-\xi^2}{2m_{\xi}^0}\right) d\xi. \quad (2.41)$$

Figure 2.5 depicts a graphical interpretation of this definition.

Typical values of ϵ arising from records of ocean waves or ship motion are less than 0.6. In practice, the statistics of maxima are calculated assuming $\epsilon \approx 0$; this gives an error of about 10% when estimating $\bar{\xi}_{1/3}$ and $\bar{\xi}_{1/10}$ (the most commonly used statistics) [133]. Consequently, the assumption of a narrow-banded wave spectrum is commonly made to evaluate the statistics related to waves and ship motion.

Using (2.41), the following quantities are defined [135, 182]:

- **Mean value of wave amplitude**

$$\bar{\zeta} = 1.5 \sqrt{m_{\zeta}^0}. \quad (2.42)$$

- **Significant wave amplitude**

$$\zeta_{1/3} = 2 \sqrt{m_{\zeta}^0}. \quad (2.43)$$

- **Significant wave height** (average of the heights of largest $1/3$ rd of the waves)

$$H_{1/3} \text{ (or } H_s) = 4 \sqrt{m_{\zeta}^0} \sqrt{1 - \frac{\epsilon^2}{1}}. \quad (2.44)$$

In practice, the significant wave height is estimated as $H_{1/3} = 4 \sqrt{m_{\zeta}^0}$. As already mentioned, for marine applications the spectral broadness is of order

0.6, and for this value, the third factor in (2.44) is 0.9055, which justifies the approximation.

The significant wave height is used to define the sea state. Table 2.1 shows the sea state code commonly used to describe the seaway in marine applications.

Table 2.1. World meteorological sea state definitions.

Sea state code	$H_{1/3}$ lower limit	$H_{1/3}$ upper limit	Seaway description
0	0	0	Calm (glassy)
1	0	0.1	Calm (rippled)
2	0.1	0.5	Smooth (wavelets)
3	0.5	1.25	Slight
4	1.25	2.5	Moderate
5	2.5	4	Rough
6	4	6	Very rough
7	6	9	High
8	9	14	Very high
9	14	>14	Phenomenal

Although here we have considered the statistics of wave elevation, the concepts apply to Gaussian narrow-banded processes in general. As we will see in the next chapters, the motion response of a vessel to the wave excitations can be considered to certain extent within a linear framework. Therefore, under the Gaussian assumption for the wave elevation and the linearity of the response, the resulting ship motion can also be considered Gaussian; and all the above statistics can also be used to characterise ship motion.

2.4.3 A Note on the Units of the Spectral Density

Very often we have to deal with spectra expressed as a function of either frequency f (Hz) or circular frequency ω (rad/s). This mix usually arises when we need to compare data from different disciplines, or when using some simulation tools. The conversion, although simple, can result in errors.

As stated by Newland [158], a way to avoid potential blunders is to note that the energy is maintained regardless of the frequency units. Thus, if $S_{\zeta\zeta}(\omega)$ and $W_{\zeta\zeta}(f)$ are spectra of the same magnitude $\zeta(t)$ expressed in different frequency units, it follows that

$$S_{\zeta\zeta}(\omega) d\omega = W_{\zeta\zeta}(f) df,$$

with $d\omega = 2\pi df$. Then,

$$S_{\zeta\zeta}(\omega) d\omega = W_{\zeta\zeta}\left(\frac{\omega}{2\pi}\right) \frac{d\omega}{2\pi},$$

which leads to

$$S_{\zeta\zeta}(\omega) = \frac{1}{2\pi} W_{\zeta\zeta}\left(\frac{\omega}{2\pi}\right).$$

Similarly,

$$W_{\zeta\zeta}(f) = 2\pi S_{\zeta\zeta}(2\pi f).$$

Another factor that could lead to erroneous results when calculating the energy from the PSD is the scaling adopted for the Fourier transform. The Wiener-Khintchine theorem establishes that the PSD $\mathbf{S}_{\zeta\zeta}(\omega)$ of a continuous-time stationary stochastic process $\zeta(t)$ and its autocorrelation function $\mathbf{R}_{\zeta\zeta}[\tau] = \mathbf{E}[\zeta(t)\zeta(t - \tau)]$ are a Fourier transform pair:

$$\mathbf{S}_{\zeta\zeta}(\omega) = c_1 \int_{-\infty}^{\infty} \mathbf{R}_{\zeta\zeta}[\tau] \exp(-j\omega\tau) \, d\tau \quad (2.45)$$

$$\mathbf{R}_{\zeta\zeta}[\tau] = c_2 \int_{-\infty}^{\infty} \mathbf{S}_{\zeta\zeta}(\omega) \exp(j\omega\tau) \, d\omega, \quad (2.46)$$

where the values of the constants c_1 and c_2 must satisfy the following condition:

$$c_1 c_2 = \frac{1}{2\pi}. \quad (2.47)$$

Typical choices are

$$c_1 = 1, \quad c_2 = \frac{1}{2\pi},$$

or

$$c_1 = \frac{1}{\pi}, \quad c_2 = \frac{1}{2}.$$

The first choice is commonly adopted in control engineering because the Laplace transform reduces to the Fourier transform when $s = j\omega$ [39]. The second choice is commonly adopted in marine technology to describe waves [163]. In this framework, the following relations hold:

$$\mathbf{var}[\zeta] = \mathbf{E}[\zeta^2] = \mathbf{R}_{\zeta\zeta}[0] = \frac{1}{2} \int_{-\infty}^{\infty} \mathbf{S}_{\zeta\zeta}(\omega) \, d\omega = \int_0^{\infty} \mathbf{S}_{\zeta\zeta}(\omega) \, d\omega. \quad (2.48)$$

One should be careful and find which one is the appropriate constant c_2 when calculating the variance by integrating a given PSD.

2.5 Standard Spectrum Formulae

After the wind has blown constantly for a certain period of time, the sea elevation can be assumed statistically stable. In this case, the sea is referred to as *fully developed*. If the irregularity of the observed waves is only in the dominant wind direction, so that there are mainly uni-directional wave crests with varying separation but remaining parallel to each other, the sea

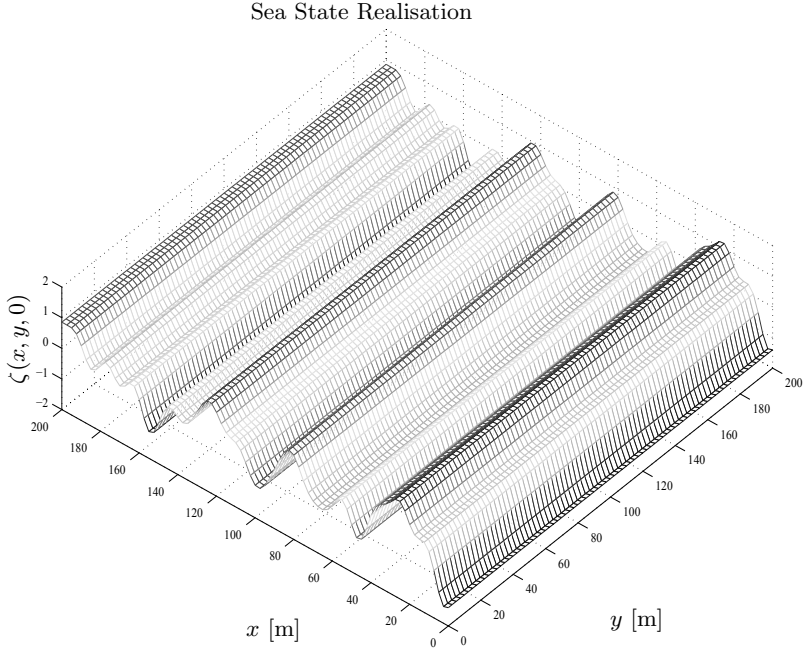


Fig. 2.6. Snapshot of a simulation of a long-crested sea.

is referred to as a *long-crested* irregular sea [182]—see Figure 2.6. If there are data available from wave ride buoys, the sea spectrum can be determined using spectral estimation techniques—see, for example, [220]. In cases where no wave records are available, standard, idealized, formulae can be used.

One family of idealised spectra is the *Bretschneider* family, which was developed in early 1950s [38]:

$$\mathbf{S}_{\zeta\zeta}(\omega) = \frac{A}{\omega^5} \exp\left(\frac{-B}{\omega^4}\right) \quad [\text{m}^2\text{s}]. \quad (2.49)$$

The parameters A and B are related to the modal frequency and the spectral moments. The modal frequency satisfies,

$$\omega_0 = \left(\frac{4B}{5}\right)^{\frac{1}{4}}, \quad (2.50)$$

where

$$\left. \frac{dS_{\zeta\zeta}(\omega)}{d\omega} \right|_{\omega=\omega_0} = 0$$

and

$$m_{\zeta}^0 = \frac{A}{4B} \quad m_{\zeta}^1 = 0.3 \frac{A}{B^{3/4}} \quad m_{\zeta}^2 = \sqrt{\frac{\pi A^2}{16B}}. \quad (2.51)$$

This family can be used to represent rising and falling seas, as well as fully developed seas with no swell² and unlimited fetch³—see [133] and references therein for further details.

In the 1960s, the *Pierson-Moskowitz* family was developed to forecast storm waves at a single point in fully developed seas with no swell using wind data [181]. This family relates the parameters A and B to the average wind speed at 19.5m above the sea surface $\bar{V}_{19.5}$:

$$A = 8.1 \times 10^{-3} g^2 \quad B = \frac{0.74g}{\bar{V}_{19.5}}. \quad (2.52)$$

The 15th International Towing Tank Conference (ITTC) in 1978 recommended the use of the *Modified Pierson-Moskowitz* family. For this family, the significant wave height and different wave period statistics are used to parameterize each spectrum:

$$A = \frac{487H_{1/3}^2}{T_0^4} = \frac{173H_{1/3}^2}{T_1^4} = \frac{123H_{1/3}^2}{T_z^4}, \quad (2.53)$$

$$B = \frac{1949}{T_0^4} = \frac{691}{T_1^4} = \frac{495}{T_z^4}.$$

Figure 2.7, shows a plot of the ITTC sea spectrum and the wave slope spectrum for a particular wave height and different wave mean periods.

There are other families that account for the case of limited fetch like the JONSWAP spectra (see [133] for [220] for this version), and also spectra that account for both wind waves and swell like the empirical double-peak Torsethaugen spectra (see [67] and references therein for details.)

²This term is commonly used to describe long wave components that are the result of storms of great intensity occurring, or that have occurred, in areas far away (order of thousand of kilometres) from the observation point. When these low-frequency components contaminate the local wind waves, double-peaked spectra need to be considered.

³*Fetch* is the distance between the point at which the waves are observed and a windward boundary, such as a shore or the edge of a storm area. The fetch gives a notion of the area of interaction between the wind and sea surface with respect to the observation point [133].

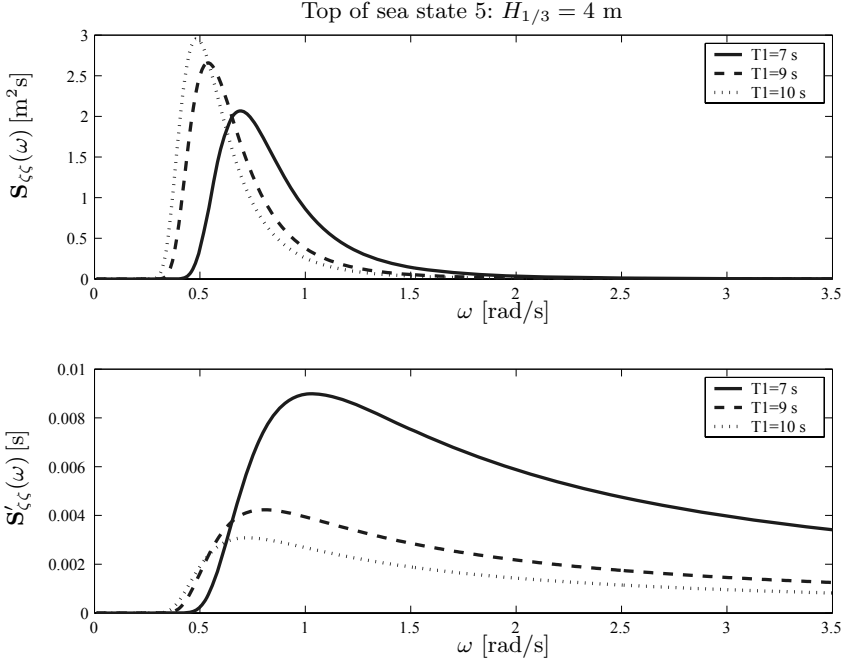


Fig. 2.7. Example of ITTC PSD for the wave elevation and wave slope for $H_{1/3} = 4$ m and $T_1 = 7, 9$ and 10 s.

2.6 Linear Representation of Long-crested Irregular Seas

If white noise⁴ w is passed through a linear filter with transfer function $H(j\omega)$, then it follows from the linearity of the filter that the PSD \mathbf{S}_{yy} of the output y is given by

$$\mathbf{S}_{yy}(j\omega) = |H(j\omega)|^2 \mathbf{S}_{ww}, \quad (2.54)$$

where \mathbf{S}_{ww} is the intensity of the white noise (constant height of the PSD.) The filter $H(j\omega)$ is called a *shaping filter* because it can be designed so that \mathbf{S}_{yy} approximates the shape of the PSD of the signal of interest. Equation (2.54) is the spectral factorization of $\mathbf{S}_{yy}(j\omega)$. This method is commonly used in control for analysis and simulation of the disturbances acting on the system (see, for example, [8], [24] or [128]), and can be used to approximate the sea spectrum.

As commented by Fossen [66], spectral factorisation methods were first applied in the marine environment to model high-frequency ship motions in dynamic positioning applications in the 1970s. Since then, several authors have

⁴A signal with constant power spectral density over all frequencies of interest.

proposed different orders and structure for the filter $H(j\omega)$ to model wave-induced motion on ships and marine structures—see, for example, [79] and [96]. The most commonly used filter to model these effects is a second-order filter of the form [66]:

$$H(j\omega) = \frac{2\xi\omega_n(j\omega)}{(j\omega)^2 + 2\xi\omega_n(j\omega) + \omega_n^2}. \quad (2.55)$$

This particular filter has the property that

$$|H(j\omega)|^2 = \frac{4(\xi\omega_n\omega)^2}{(\omega_n^2 - \omega^2)^2 + 4(\xi\omega_n\omega)^2}; \quad (2.56)$$

and then,

$$\max_{\omega} \mathbf{S}_{yy} = |H(j\omega)|^2 \mathbf{S}_{ww} = \mathbf{S}_{nn}. \quad (2.57)$$

To approximate a given spectrum, the parameters of the filter can be chosen according to the following rules:

- 1- The intensity of the noise driving the filter is obtained from

$$\mathbf{S}_{ww} = \max_{\omega} \mathbf{S}_{yy}(\omega). \quad (2.58)$$

- 2- The natural frequency of the filter is obtained from

$$\omega_n \approx \arg \max_{\omega} \mathbf{S}_{yy}(\omega). \quad (2.59)$$

- 3- The damping coefficient $0 < \xi < 1$ is calculated such that the variance of the output of the filter matches the variance of the original spectrum, *i.e.*

$$\int_0^{\infty} |H(\xi, \omega)|^2 \mathbf{S}_{ww} d\omega \approx m_y^0. \quad (2.60)$$

The last equation can be solved using a simple bi-section algorithm [41]. Equation (2.60) ensures that the energy of the approximation equals the energy of the spectrum being approximated.

A state-space representation of (2.55) that can be used for time domain simulations is

$$\begin{aligned} \begin{bmatrix} \dot{x}_1 \\ \dot{x}_2 \end{bmatrix} &= \begin{bmatrix} 0 & 1 \\ -\omega_n^2 & -2\xi\omega_n \end{bmatrix} \begin{bmatrix} x_1 \\ x_2 \end{bmatrix} + \begin{bmatrix} 0 \\ 2\xi\omega_n \end{bmatrix} w, \\ y &= [0 \ 1] \begin{bmatrix} x_1 \\ x_2 \end{bmatrix} \end{aligned} \quad (2.61)$$

2.7 The Encounter Spectrum

When a ship is moving with a certain speed, the frequencies observed from the ship differ from those observed in a stationary frame: the frequencies change according to (2.29). This Doppler effect changes not only the frequency range of the spectrum but also its shape. The wave spectrum seen from the ship is called the *wave encounter spectrum* $\mathbf{S}(\omega_e)$.

Since the power of any magnitude is invariant with respect to the reference frame from which it is observed, for any PSD the following holds:

$$\mathbf{S}(\omega_e) d\omega_e = \mathbf{S}(\omega) d\omega.$$

From this, it follows that

$$\mathbf{S}(\omega_e) = \frac{\mathbf{S}(\omega)}{\left| \frac{d\omega}{d\omega_e} \right|} = \frac{\mathbf{S}(\omega)}{\left| 1 - \frac{2\omega U}{g} \cos(\chi) \right|}. \quad (2.62)$$

For beam seas, the transformation is trivial, *i.e.* since $\cos(\pi/2) = 0$, then $\mathbf{S}(\omega_e) = \mathbf{S}(\omega)$. In bow seas, the encounter spectrum is a spread version of the wave spectrum shifted towards higher frequencies. For quartering and following seas the situation becomes complex since expression (2.62) is singular at $\bar{\omega}_w = g/(2U \cos \chi)$ where the denominator vanishes, and also because the transformation from the wave frequency to the encounter frequency is not one to one.

Figure 2.8, shows a schematic representation of the transformation in quartering seas from a particular PSD $\mathbf{S}(\omega)$ to the corresponding encounter PSD $\mathbf{S}(\omega_e)$. In this figure, the absolute value of the transformation ω to ω_e has been taken.

From Figure 2.8, we can see that the energy at low encounter frequency usually arises from the energy of three different frequency ranges in the wave frequency domain. This is depicted by the area A_{e1} . Moreover, a large amount of energy corresponding to the wave frequencies close to $\bar{\omega}$ is mapped into a small range of encounter frequencies. This effect, depicted by A_{e2} , can often result in an integrable singularity—see [182].

2.8 Short-crested Irregular Seas

When irregularities are apparent along the wave crests at right angles to the direction of the wind, the sea is referred to as *short crested* or *confused* [182]—see Figure 2.9. In this case, the waves propagate in different directions with a dominant direction (spreading). This is the most likely situation encountered at sea. As commented by Lloyd [135], a wave spectrum derived from data recorded at sea, at a particular point, will invariably contain contributions from different directions, but in most applications this can be ignored (and

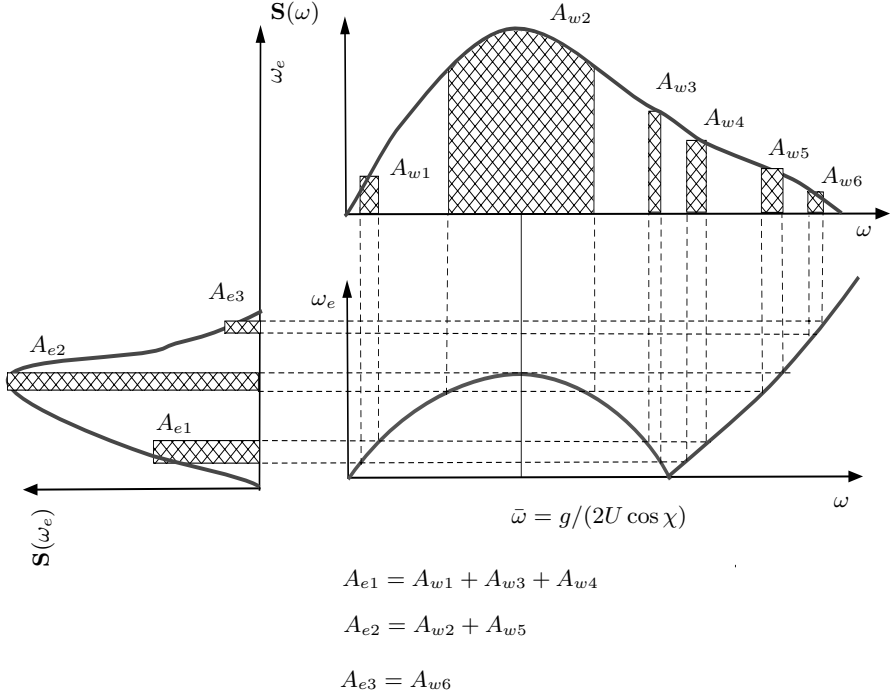


Fig. 2.8. Schematic transformation between wave and encounter frequency domain PSD in quartering and following seas.

considered that the sea is described by a long-crested sea). For example, Figure 2.13 shows simulated time series of a long-crested and a short-crested sea, but both could be considered realisations of a sea described by a long-crested spectrum. Nevertheless, the degree of spreading is important to describe ship motions due to wave loads because the response depends on how much energy there is at the different encounter angles.

For simulation and analysis purposes, it is a common practice to consider the directional spectrum as a product of two functions:

$$S_{\zeta\zeta}(\omega, \chi) = S(\omega)M(\chi), \quad (2.63)$$

where the function $M(\chi)$ is the so-called spreading function. This function, as its name indicates, spreads the energy of the spectrum $S(\omega)$, and hence the following relation is satisfied [213]:

$$m_{\zeta}^0 = \int_0^{\infty} \int_{-\pi}^{\pi} S_{\zeta\zeta}(\omega, \chi) d\chi d\omega = \int_0^{\infty} S(\omega) d\omega. \quad (2.64)$$

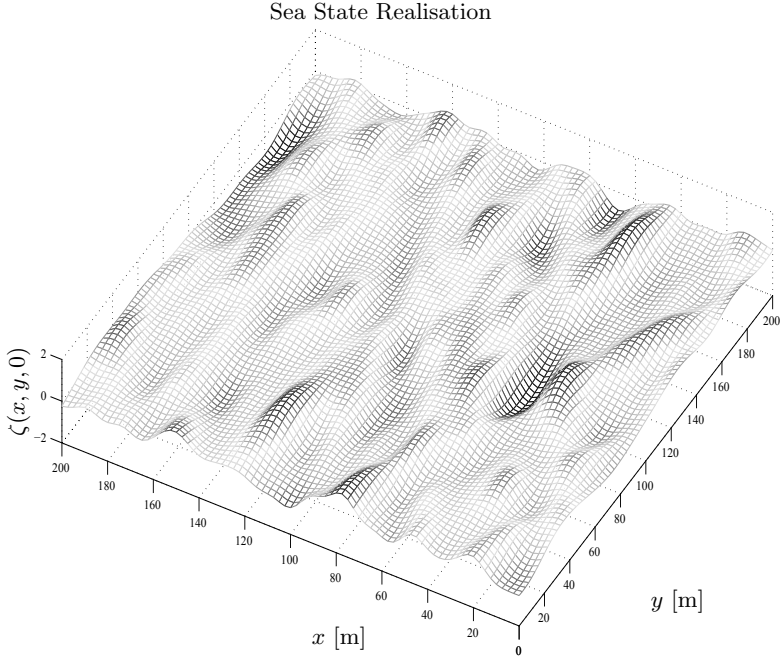


Fig. 2.9. Snapshot of a simulation of a short-crested sea.

A commonly used spreading function is of the form [155]:

$$M(\chi) = \begin{cases} \frac{2^{(2n-1)} n! (n-1)!}{\pi (2n-1)!} \cos^{2n}(\chi - \chi_0) & \text{for } -\frac{\pi}{2} < \chi - \chi_0 < \frac{\pi}{2}, \\ 0 & \text{otherwise.} \end{cases} \quad (2.65)$$

where χ_0 is the dominant wave propagation direction, and the values of $n = 1, 2$ are commonly used. See [135] for a more general form where $|\chi - \chi_0| < \alpha$; with α not necessarily equal to $\pi/2$. Figure 2.10 shows a plot of (2.65) for $n = 1, 2, 3$. Note that the higher the value of n , the larger the concentration of energy around the main direction of wave propagation. Finally, Figure 2.11 shows an example of a directional spectrum based on the ITTC spectrum and $n = 2$.

2.9 Long-term Statistics of Ocean Waves

In the previous sections, we have seen that the sea spectrum can be parameterised in terms of the significant wave height and the wave period. The sea

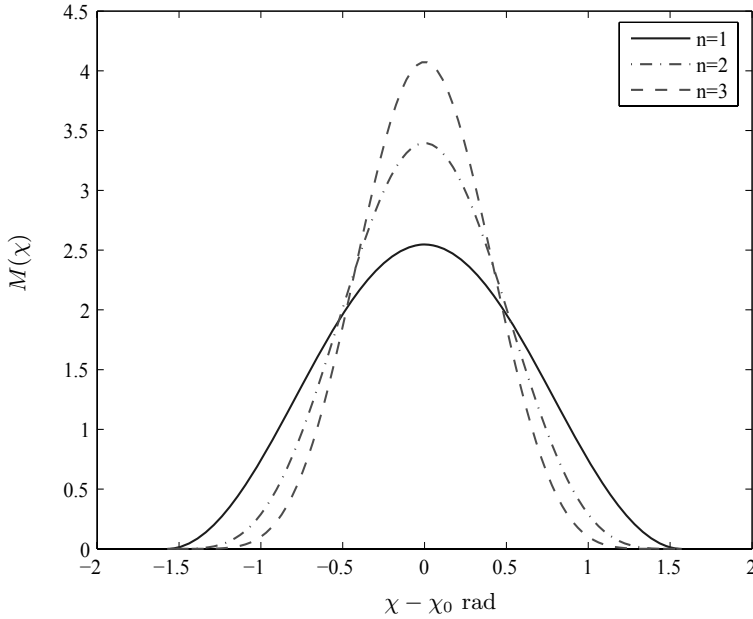


Fig. 2.10. Example of spreading function for commonly used values of n .

spectrum and all the statistics, which can be derived from it, are called *short-term statistics* because they can be used to describe the properties of the sea environment only for minutes or hours at most.

The so-called long-term statistics, by contrast, describe the probability occurrence of a particular wave height and wave period at a particular location and for a particular time of the year. These data are used to find values of wave height and period relevant to the region of operation of a particular ship. As an example, consider the data for the south-east Indian Ocean shown in Table 2.2. Similar data for different areas can be found in [107].

2.10 Simulation of Wave Elevation

As we have seen, the sea surface elevation can be considered an aperiodic wave system having a continuous energy spectrum. Using this representation, if $\zeta(t)$ is stationary on time interval $[0, T]$, its realisations can be approximated to any degree of accuracy by [186]

$$\zeta(t) = \sum_{n=1}^N \bar{\zeta}_n \cos(\omega_n t + \varepsilon_n), \quad (2.66)$$

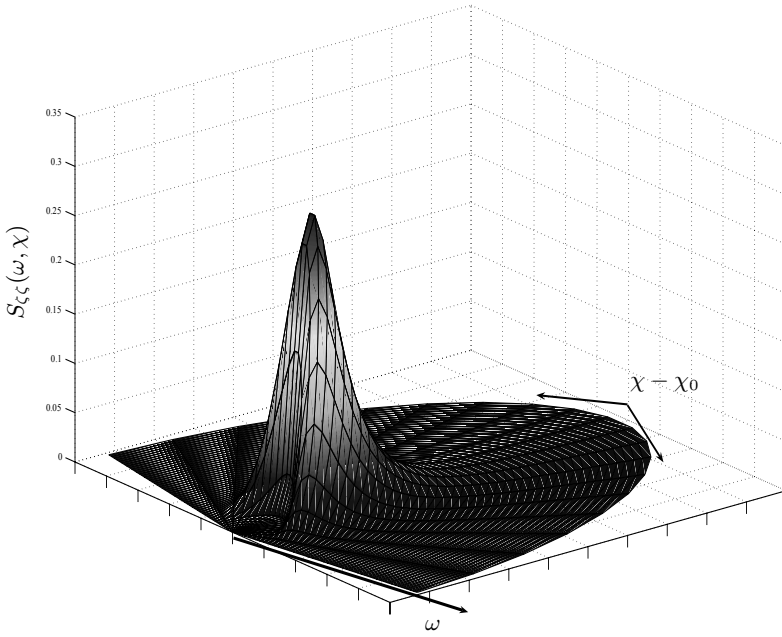


Fig. 2.11. Example of directional spectrum based on the ITTC spectrum for significant wave height of 2 m, peak frequency of 1 rad/sec and spreading with $n = 2$.

with N being sufficiently large, where $\bar{\zeta}_n$ are constants, and the phases ε_n are independent identically distributed random variables with uniform distribution in $[0, 2\pi]$. This choice of random phases ensures that $\zeta(t)$ is a Gaussian process [84, 186, 213]. This sum represents an ensemble of realisations of the process.

The autocorrelation of the process defined above is given by (see [97] for details)

$$\mathbf{R}_{\zeta\zeta}(\tau) = \mathbf{E}[\zeta(t)\zeta(t + \tau)] = \sum_{n=1}^N \frac{\bar{\zeta}_n^2}{2} \cos(\omega_n \tau). \quad (2.67)$$

Since the autocorrelation for $\tau = 0$ gives the energy of $\eta(t)$, it follows that

$$\int_0^\infty \mathbf{S}_{\zeta\zeta}(\omega) d\omega \approx \sum_{n=1}^N \frac{\bar{\zeta}_n^2}{2}, \quad (2.68)$$

and we can write

Table 2.2. Long-term statistics: wave height and wave period joint probability distribution. Area 100 south-east Indian Ocean. Reproduced from [185] and published with permission of the Director of Navy Platform Systems (DNPS), Department of Defence, Australia.

$H_{1/3}[\text{m}], T_z[\text{s}]$	< 4	4-5	5-6	6-7	7-8	8-9	9-10	10-11	11-12	12-13	>13
>14									0.1	0.1	
13-14									0.1		
12-13								0.1	0.1		
11-12							0.1	0.1	0.1		
10-11						0.1	0.1	0.1	0.1	0.1	
9-10						0.1	0.2	0.3	0.2	0.1	
8-9						0.2	0.4	0.5	0.3	0.1	
7-8					0.1	0.4	0.8	0.8	0.5	0.2	0.1
6-7					0.2	0.9	1.6	1.3	0.7	0.2	0.1
5-6			0.1	0.7	2.1	2.9	2.1	0.9	0.3	0.1	
4-5			0.2	1.7	4.4	4.8	2.8	1.0	0.3	0.1	
3-4			0.7	4.0	7.5	6.2	2.8	0.8	0.2		
2-3			0.1	2.0	7.0	8.5	4.9	1.6	0.3	0.1	
1-2			0.5	3.2	5.8	3.9	1.3	0.3			
0-1		0.1	0.4	0.9	0.6	0.2					

$$\sum_{n=1}^N \int_{\omega_n - \Delta\omega/2}^{\omega_n + \Delta\omega/2} \mathbf{S}_{\zeta\zeta}(\omega) d\omega = \sum_{n=1}^N \frac{\bar{\zeta}_n^2}{2}, \quad (2.69)$$

and take

$$\frac{\bar{\zeta}_n^2}{2} = \int_{\omega_n - \Delta\omega/2}^{\omega_n + \Delta\omega/2} \mathbf{S}_{\zeta\zeta}(\omega) d\omega = \mathbf{S}_{\zeta\zeta}(\omega^*) \Delta\omega \quad (2.70)$$

for some

$$\omega^* \in [\omega_n - \frac{\Delta\omega}{2}, \omega_n + \frac{\Delta\omega}{2}].$$

The later follows from the mean-value theorem for integrals of continuous functions under the assumption that $\mathbf{S}_{\zeta\zeta}(\omega)$ is continuous. From (2.70), it follows that

$$\bar{\zeta}_n = \sqrt{2\mathbf{S}_{\zeta\zeta}(\omega^*) \Delta\omega}. \quad (2.71)$$

In practice, small errors are incurred if we take $\omega^* = \omega_n$. Nevertheless, since the value of N is finite, one should bear in mind that we are approximating the realisation of a stochastic process by a finite sum of periodic signals, which is periodic. Indeed, if $\omega^* = \omega_n$, the realisation will repeat itself after after $2\pi/\Delta\omega$. By choosing ω^* randomly within the interval $[\omega_n - \frac{\Delta\omega}{2}, \omega_n + \frac{\Delta\omega}{2}]$, the fundamental period is increased. Therefore, the following steps can be applied, in some cases, to determine the appropriate number of sinusoids:

1. If a simulation requires $Tsim$ seconds, choose

$$\Delta\omega < \frac{2\pi}{Tsim}.$$

2. The number of sinusoids will then depend on the range of frequencies over which the spectrum is significant. If the energy is negligible outside the frequency range $[\omega_{min}, \omega_{max}]$, then one can take

$$N > \frac{(\omega_{max} - \omega_{min})}{\Delta\omega}.$$

3. Choose ω^* random in each interval $[\omega_n - \frac{\Delta\omega}{2}, \omega_n + \frac{\Delta\omega}{2}]$ to ensure that the fundamental period of the realizations is larger than $Tsim$.

This is summarised in Figure 2.12.

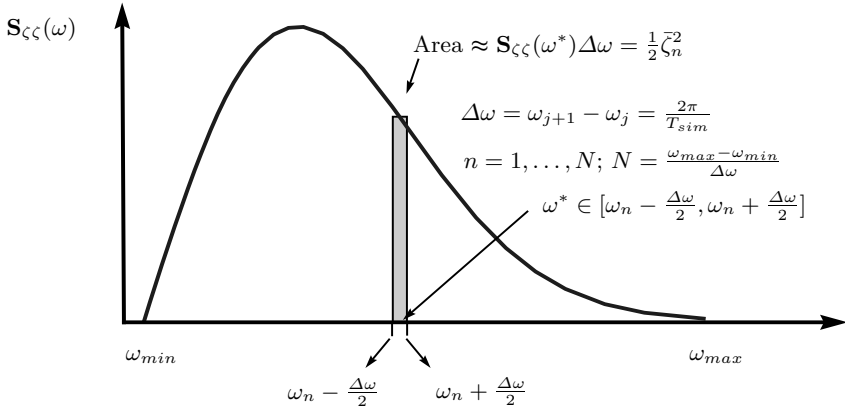


Fig. 2.12. Obtention of regular component amplitudes for time series simulations.

Using the results given above, we can then generate the time series for numerical simulations as follows:

- for long-crested seas:

$$\zeta(x, y, t) = \sum_{n=1}^N \sqrt{2S_{\zeta\zeta}(\omega^*)\Delta\omega} \cos(\omega^*t + \varepsilon_n - k_n(x \cos \chi - y \sin \chi)), \quad (2.72)$$

with ω^* taken randomly in each interval $[\omega_n - \frac{\Delta\omega}{2}, \omega_n + \frac{\Delta\omega}{2}]$.

- for short-crested seas:

$$\zeta(x, y, t) = \sum_{n=1}^N \sum_{m=1}^M \sqrt{2S_{\zeta\zeta}(\omega^*, \chi^*)\Delta\omega\Delta\chi} \cos(\omega^*t + \varepsilon_{n,m} - k_n(x \cos \chi_m - y \sin \chi_m)). \quad (2.73)$$

with ω^* and χ^* taken randomly in each of the intervals $[\omega_n - \frac{\Delta\omega}{2}, \omega_n + \frac{\Delta\omega}{2}]$ and $[\chi_m - \frac{\Delta\chi}{2}, \chi_m + \frac{\Delta\chi}{2}]$ respectively.

Figures 2.6, 2.9 and 2.13 show the numerical results of expressions (2.72) and (2.73) for a simulation example. In this example, we have used the ITTC spectrum with significant wave height of 2 m and modal period of 1 rad/s. Figure 2.6 shows a snapshot of the sea surface elevation for the long-crested case, whereas Figure 2.9 shows the results for the short-crested case. The latter was obtained using the spreading function with spreading factor $n = 2$. Figure 2.13 shows the corresponding time series at the location $x = 0, y = 0$.

As commented at the beginning of Section 2.8, if we derive a wave spectrum from the data of a particular point (for example, using the data shown in Figure 2.13), the directionality can be ignored in most applications, and we could consider that the sea is described by a long-crested sea. This is clear from the two realisations shown in Figure 2.13; both could be considered realisations of a sea described by a long-crested spectrum. However, as we will see in Chapter 4, the degree of spreading is important to describe ship motion.

Similar results can be obtained using the linear approximations presented in Section 2.6. In the case of long-crested seas, we simply have to filter white noise. For the short-crested case, however, we need to tune as many shaping filters as there are directions being considered. Hence, the simplicity of the linear method for this case can be argued.

Finally, in the case of simulation in the encounter frequency domain, for the case of a ship moving with forward speed, expressions (2.72) and (2.73) remain valid by substituting ω^* by ω_e^* and the corresponding wave numbers k_e . In the case of using linear approximations, the directions need to be discretised and then the filters need to be tuned for each encounter spectrum. We shall

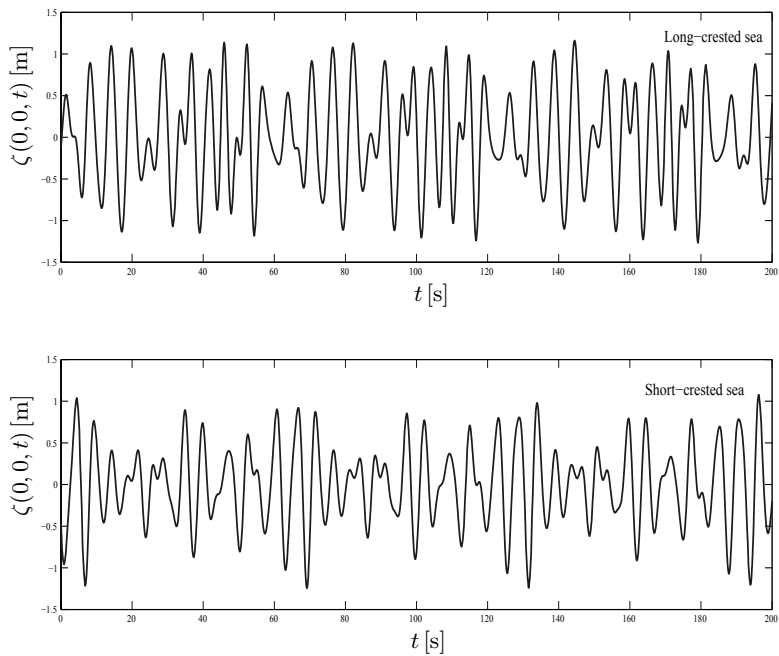


Fig. 2.13. Time series at the origin for an ITTC spectrum for significant wave height of 2 m, peak frequency of 1 rad/s. Long crested (top plot); short crested for 10 directions with spreading factor $n = 2$ (bottom plot.)

see, in the second part of the book, that the latter is a useful analysis tool for the study of performance limitations.

<http://www.springer.com/978-1-85233-959-3>

Ship Motion Control
Course Keeping and Roll Stabilisation Using Rudder and
Fins

Perez, T.

2005, XXI, 300 p., Hardcover

ISBN: 978-1-85233-959-3